Automated Detection of Surface Defects on Razor Blades through Video Analysis

Lilong Chen 1,2,*

1 Department of Digital Media Technology, Sanming University, Sanming 365004, China

2 Faculty of Humanitarian Education, Krasnodar State Institute of Culture, Krasnodar 350072, Russia

* Correspondence: 20151102@fjsmu.edu.cn; Tel.: +86-180-6590-1853

Abstract: In the manufacturing process of razor blades, the presence of surface defects directly impacts their quality and lifespan. Manual detection of these defects is not only inefficient but also susceptible to external interference. To achieve real-time and stable detection of blade defects, a method based on video analysis was proposed in this paper. Raw surface images of the blades were captured using a computer vision system, and binarization was performed using Otsu's algorithm. Subsequently, contours were identified and preliminarily analyzed using the CCL algorithm to obtain Regions of Interest (ROI). The ROI was then sorted, and subtle defects were filtered out through morphological analysis. A mask was obtained by comparing the ROI with a background model constructed based on frame averaging. Through mask analysis, defect types were determined, achieving efficient detection of surface defects on razor blades. Experimental results demonstrated that the proposed method enabled real-time detection of multiple defect types simultaneously.

Keywords: Razor blades; surface defect detection; video analysis; computer vision

1. Introduction

The mechanical processing steps of razor blade production include cutting and pressing. Due to factors such as material characteristics and mechanical performance, surface defects like scratches and damage easily occur on the blades. The emergence of these defects significantly impacts the quality and performance of the products, making their detection crucial. While human eyes can relatively easily perceive some minor defects, especially those with texture features, manual inspection poses challenges in terms of time, effort, and is constrained by factors like labor costs and working hours.

Utilizing machine vision technology for defect detection offers a solution to save considerable time and labor costs, enabling automation and pipeline operations in the production process. This approach efficiently addresses small defects, especially those with texture features, enhancing product quality and performance. Therefore, introducing machine vision technology for automated defect detection can effectively improve production efficiency, reduce human errors, and bring higher economic benefits to the manufacturing industry.

Research on blade detection technology is extensive and widely applied in the field of machine vision, with many scholars conducting in-depth studies. In terms of image acquisition and processing, researchers are implementing various techniques: You et al. [1] reduce machine downtime for milling tool single-frame capture by using gradient time series and a classification model to identify continuous image frames and track tool wear based on wear characteristics and local search. Guo et al. [2] capture clear images of micro-milling cutter contours, designing a remote-centered backlight illuminator to effectively mitigate the influence of tool thickness. Ji et al. [3] employ a segmented acquisition and stitching method to obtain images of large-length

U-shaped steel, enabling visual inspection of workpieces. Coronadob et al. [4] describe wear image surface features using directional gradient histograms and train classifiers to identify and classify abrasive surface wear images. Hou et al. [5] use prisms to simultaneously capture bottom and side edges, acquiring geometric parameters of cutting tools through connected domains and outer rectangles, and finally fitting cutting edge wear using the least squares method. In the detection system design, Wang et al. [6] develop a machine vision-based online tool wear detection system supporting human-machine interaction. Zou et al. [7] reduce the impact of detail information on circular lithium battery pole piece cutting tool edge detection by using a backlight illumination scheme and segmenting least squares fitting and radius-constrained circular arc fitting for contour reconstruction. Cui et al. [8] achieve image registration and fusion under limited camera field of view, obtaining complete side-cut rectangular unfolded images of micro-drills in one shot. Jing et al. [9] utilize topological descriptors combined with gray-level co-occurrence matrices to extract surface texture for recording machine tool cutting tool wear, and integrate feature data with genetic algorithms to train linear classifiers for wear classification. Ye et al. [10] design a clean, integrated online monitoring system for detecting cutting edge wear in the presence of oil and dust interference, reconstructing worn blade tips by fitting straight lines to contour edges, and calculating wear amounts by subtracting reconstructed before and after images, with experimental verification showing that this contour reconstruction method effectively improves wear detection accuracy.

In the realm of edge detection and contour extraction for blade inspection, various methodologies have been proposed by different researchers. Zhu et al. [11] propose a region-growing method based on MCA to differentiate backgrounds and extract worn areas in low-quality micro-milling cutter wear images with noise and blurred boundaries. You et al. [12] utilize sharpened milling tool histogram for region localization and employ the GrabCut algorithm for wear area extraction, followed by calculating wear area through least squares fitting of cutting edge edges. Bagga et al. [13] employ fuzzy logic to detect binary numerical control lathe tool edge data, training degradation models to predict tool lifespan. Although this predictive algorithm can monitor tool wear status in real-time, it requires extensive data support and long training times with high computational overhead. Wan et al. [14] propose a precise adaptive segmentation method combining U-Net with regions of interest for identifying pyramid-shaped abrasive images and inferring wear evolution through shape parameter calculation. Chen [15] improves the processing of numerical control machine tool image contour features using optimized Gaussian interpolation sub-pixel edge detection, reducing the number of iterations in contour extraction, and a dual-angle point detection method to measure tool straightness, length, and angle. However, the effectiveness of this detection method relies heavily on the presence of special points in the tool contour features, which may limit its applicability. Liang et al. [16] achieve machine vision detection of micrometer-level notches in battery pole cutting edges using micrograph images, employing ARNet to remove edge attachments, Zernike moments to detect sub-pixel edges, and a region-growing method capable of selecting growing points and merging adjacent areas based on certain conditions to detect defect notches. Cheng et al. [17] implement online detection of circular diamond turning tool tips using coaxial eccentric lenses, detecting and extracting sub-pixel accuracy arc-shaped tool edge using Zernike moments, and performing least squares fitting on extracted edge contours to obtain positioning information. Liu et al. [18] propose a detection scheme centered around edge extraction for metal parts with indistinct

defect boundaries, extracting contours by skeletonizing pre-processed images, fitting them into multiple edge line segments, and reconstructing edge line segments by removing outliers based on local average gray values after traversing the largest class of line segment coordinate point sets based on direction vectors. Zhu [19] improves defect extraction accuracy for weak metal surface defects by removing background and reflective areas through threshold segmentation and edge detection, removing holes and logos based on connected domain area, enhancing detail information using homomorphic filtering, and obtaining texture saliency maps through saliency detection algorithms. Wang et al. [20] introduce a twin dense branch network based on multi-scale feature segmentation for accurate segmentation and recognition of metal surface defects. Xu et al. [21] implement rapid matching of template images with defect differences in detection images using a shape template matching algorithm combined with a pyramid algorithm, and design a circular fitting contour method to accurately locate small areas of circular tool tips for tool shape detection. Hu et al. [22] use the Roberts edge detection method based on the difference in grayscale values in two perpendicular directions for contour extraction. Yu et al. [23] introduce grayscale interpolation before and after filtering into Gaussian smoothing to retain image details, using the ratio of average variance to grayscale as the dual threshold for the improved Canny operator. Wang et al. [24] propose a combination of the Otsu segmentation and Canny algorithms for contour detection of micro-drill bits, followed by filtering of corner detection and feature matching algorithms for product contour selection.

This paper detailed a research endeavor aimed at developing an innovative system for identifying defects on the surface of razor blades. The primary goal was to establish a system that seamlessly operated within industrial conditions, enabling the inspection of all razor blades entering the production line. The pivotal objective was the identification and subsequent rejection of defective razor blades, with the ultimate aim of enhancing the overall quality of the final product. This strategic approach was designed to preemptively eliminate the need for repairing finished products that may incorporate defective blades, thereby mitigating associated costs.

Given the dynamics of the production cycle, the imaging process for razor blade surfaces was not to exceed 1 second. Furthermore, the analysis and identification of defective razor blades needed to be completed in less than 1 second. Additionally, the system was anticipated to accurately determine the dimensions of the razor blades captured in the image during the inspection process.

To achieve this ambitious goal, the research involved the development of an innovative imaging methodology that facilitated the continuous inspection of razor blade surface quality in a flow-through mode. This implied that the razor blades were not halted in the production line; instead, they moved along a conveyor belt, and an image of the surface was captured during their continuous movement. Subsequently, the captured image underwent thorough analysis, culminating in a surface evaluation result. This result was then utilized by the sorting system to facilitate the prompt removal of defective razor blades from the production process. This research contributed to an overarching project dedicated to advancing manufacturing quality by eliminating the use of defective razor blades.

2. Materials and Methods

To meet the demands of practical industrial applications, an intelligent sorting system has been developed, integrating rapid dynamic detection and sorting of razor blades to achieve

efficient quality sorting. In the context of industrialization, machine vision technology was employed to dynamically identify surface scratches and damages on razor blades. Ensuring image quality was paramount, and for this purpose, the M1620-MPW2 industrial camera lens from Computar was selected, featuring a 16mm focal length, a minimum object distance of 20cm, and a resolution of 5 million pixels. The industrial camera chosen was the MER-531-20GC-P model from DAHENG IMAGING, equipped with a 1-inch PYTHON5000 Global shutter CMOS sensor chip, integrated with a Gigabit Ethernet interface, supporting color spectrum, and suitable for challenging working environments. LED spotlighting was employed as the light source.

A platform for capturing images of the razor blade surface was designed (see Figure 1). During the image capture process, adjustments were made to the distance and angle between the light source and conveyor belt, as well as the working distance and aperture size of the camera, to find the optimal positions for the light source and camera, ensuring high-quality images of the razor blade surface. In practical shooting scenarios, the camera was installed in a dark box located on the conveyor belt, with LED spotlighting providing a stable illumination environment, ensuring the stability of image quality. Such configurations and designs were aimed at achieving high-speed and efficient detection and sorting of razor blade defects.

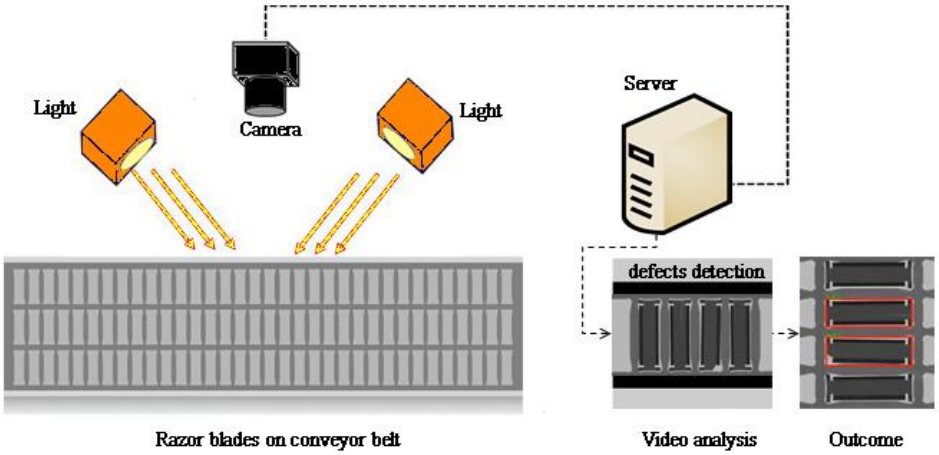

Figure 1. Razor blade surface defect detection platform.

In addressing the issue of surface defect detection on razor blades, it was necessary to construct a razor blade template model for continuous processing of video sequences, serving as a reference in defect detection analysis. Given the relative stability of parameters, including raw materials and lighting conditions, in the entire detection system over a certain period, and considering computational costs and memory requirements, a non-recursive frame averaging method was employed in this study to build the razor blade template model. However, it was imperative that the razor blades used for constructing the template model were defect-free, and their differences minimized as much as possible. The effectiveness of razor blade defect detection is highly contingent on the quality of the background model constructed. The definition of the razor blade template model based on frame averaging is provided below.

$$M(x, y) = \sum_{i=1}^{n} F_i(x, y) \Big/ n \qquad (1)$$

Where n represents the number of frames used to construct the template model for razor

blades, and $F_i(x, y)$ denotes a frame in the video sequence.

The non-recursive frame averaging method has the advantage of low computational cost; however, its drawbacks include sensitivity to changes in lighting conditions and conveyor belt speed. The razor blade template model constructed using the non-recursive method needs updating based on variations in raw materials, product batches (different models), or environmental parameters. In a closed production workshop, where the illumination for the test objects remains constant, and the conveyor belt moves at a speed of 0.2 m/s.

In order to better assess the effectiveness of the system, the proportion of defective razor blades was intentionally increased. Each frame obtained at regular intervals from the video sequence underwent a preprocessing procedure (see Figure 2). The central part of the video sequence frames, the Region of Interest (ROI), was extracted. The images within the ROI were binarized, followed by contour detection and analysis to determine the position of each blade. The positions of each blade were sorted from top to bottom. Subsequently, the differential binarized image was calculated based on the binarized template model. Contour analysis was performed on the differential binarized image(mask) to eliminate edge differences, identifying defects such as scratches and damage.

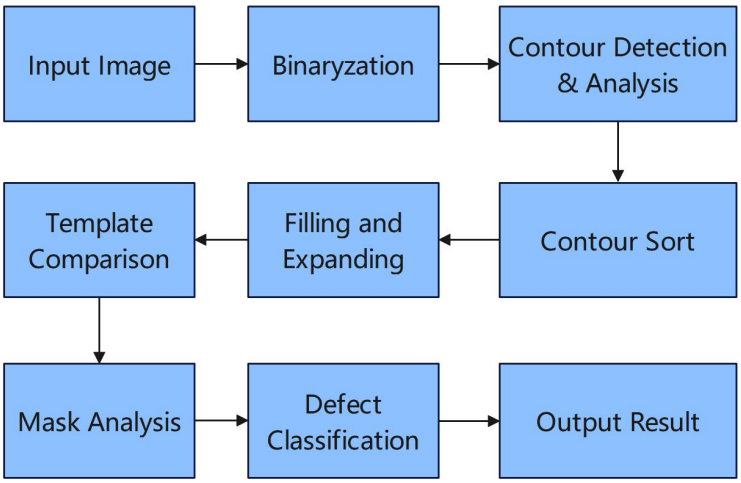

Figure 2. Preprocessing Workflow for Razor Blade Video Frames.

The specifications of razor blades in the same batch are identical. In Figure 3, an array of razor blade frames (partial) captured by the camera, it can be clearly observed, through visual inspection, that the first, third, and fourth razor blades (from top to bottom) have noticeable defects. These defects include not only scratches (third blade) but also damages (first and fourth blades). No apparent defects were found in the others.

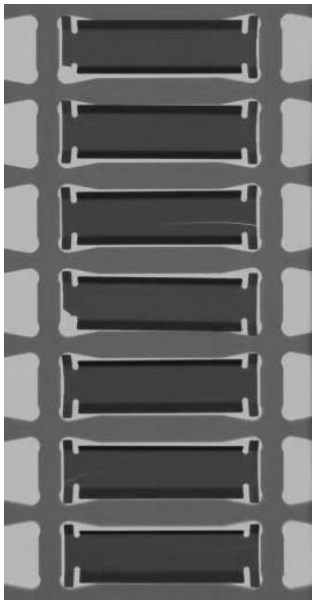

Figure 3. A Partial Array of Captured Razor Blades by the Camera.

According to the NTSC Luminance Equation (see Equation 1), Figure 3 was transformed into a grayscale image. There are various methods for threshold calculation in grayscale image binarization. From the perspective of algorithm types, these methods can be broadly classified into global thresholding and local thresholding. In this study, the global thresholding method known as Otsu's method was employed (see Equations 2 to 8) [25-26]. This method is primarily based on the information from the grayscale histogram of the image. It calculates the minimum intra-class variance to find the threshold value (T), which is used to separate the image into foreground (white) and background (black). The grayscale values of the image range from 0 to 255. A loop is required to calculate the intra-class variance for each grayscale value used as a threshold. The final threshold value is determined by selecting the grayscale value that corresponds to the minimum intra-class variance, resulting in image binarization (see Figure 4).

$$\mathrm{L(x,y)} = 0.299 * \mathrm{R_{(x,y)}} + 0.587 * \mathrm{G_{(x,y)}} + 0.144 * \mathrm{B_{(x,y)}} \quad (2)$$

$$\omega_b(t) = \sum_{i=0}^{t-1} p(i) \quad (3)$$

$$\mu_{\mathrm{b}}(\mathrm{t}) = \sum_{\mathrm{i}=0}^{\mathrm{t}-1} ip(i) \Big/ \omega_b(t) \quad (4)$$

$$\sigma_b^2 = \sum_{i=0}^{t-1} [i - \mu_{\mathrm{b}}(\mathrm{t})]^2 p(i) \Big/ \omega_b(t) \quad (5)$$

$$\omega_f(t) = \sum_{i=t}^{L-1} p(i) \quad (6)$$

$$\mu_{\mathrm{f}}(\mathrm{t}) = \sum_{\mathrm{i}=0}^{\mathrm{L}-1} ip(i) \Big/ \omega_f(t) \quad (7)$$

$$\sigma_f^2 = \sum_{i=t}^{L-1} [i - \mu_f(t)]^2 p(i) \Big/ \omega_f(t) \quad (8)$$

$$\sigma_w^2(t) = \omega_b(t)\sigma_b^2(t) + \omega_f(t)\sigma_f^2(t) \quad (9)$$

In this context, ω_b represented the proportion of background pixels, σ_b^2 denoted the variance of background pixels, ω_f indicated the proportion of foreground pixels, and σ_f^2 signified the variance of foreground pixels. They were the probabilities and variances of two classes separated by the threshold.

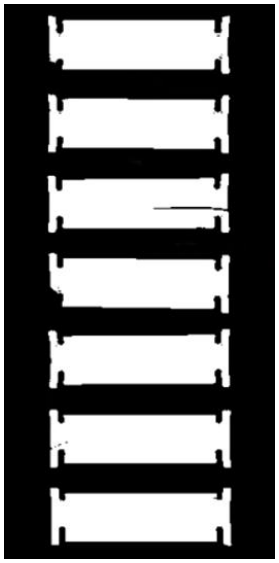

Figure 4. Binarized razor blade array.

In order to control the defect rate in industrial production without significantly affecting product lifespan and within acceptable limits for consumers, it is necessary to strike a balance between actual production costs, process requirements, and other factors when scientifically formulating inspection standards. Setting overly stringent inspection standards may lead to an increase in the defective product rate, subsequently raising production costs and the difficulty of meeting process requirements, which will ultimately be reflected in the product's selling price. Moreover, excessively strict standards may also impact the effectiveness of defect detection.

In Figure 4, the naked eye can discern extremely subtle spots on the right side of the first blade and a band of extremely subtle spots on the left side of the fifth blade. For such extremely subtle defects (which may also be interference information), morphological opening operations can be employed to fill in gaps during the analysis of video frames, as shown in Figure 5. From Figure 5, it can be observed that the extremely subtle spots on the right side of the first blade and the band of extremely subtle spots on the left side of the fifth blade have both disappeared.

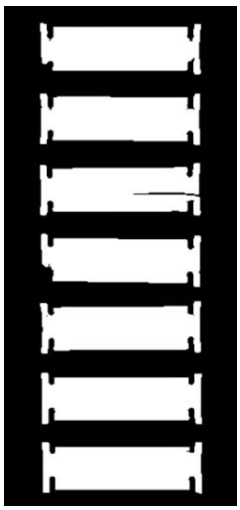

Figure 5. The razor blade array after morphological opening operation.

Based on the CCL (Connected Component Labeling) algorithm, this paper extracted the edges of each object and all its sub-objects in the binary image (Figure 5). By calculating the aspect ratio of the maximum bounding rectangle of the contours and filtering out the black background, we were able to eliminate unwanted elements. Additionally, through the computation of the area of the maximum bounding rectangle (with an area threshold set to 150 in this study), we successfully filtered out small contours within each white region. The result was the acquisition of white contours representing razor blades (see Figure 6).

After calculating the y-coordinate values of the top-left corner of each contour, we sorted them in ascending order and labeled the sequence numbers at the top-left corner of each contour (see Figure 7).

Figure 6. Contour discovery and contour analysis.

Figure 7. Contour sorting.

Subsequently, the binary template model was computed against the difference binary images of each contour (ROI) (see Figure 8). Contour analysis was performed on these difference binary images to eliminate edge differences and accurately identify defects such as scratches and damages.

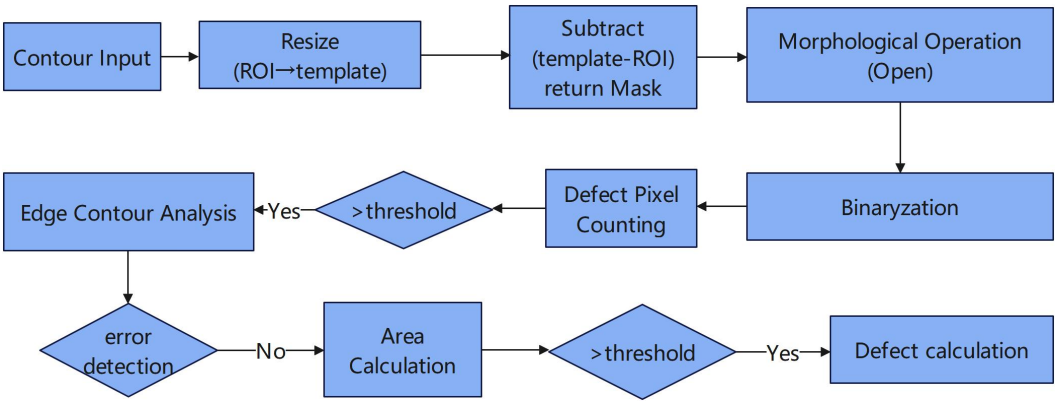

Figure 8. Template comparison and defect type identification.

The algorithm for template matching and defect type recognition is as follows:

(1) Adjust the contour size to match that of the binarized template model;

(2) Calculate the difference binary image (Mask) between the binarized template model and each contour (ROI) (see Figure 9). From Figure 5, it can be observed that in the difference binary image of the first blade, there is a white area in the lower-left corner, indicating a defect of breakage, and a small white area in the upper-right corner that needs to be filtered through a threshold. In the difference binary image of the third blade, a distinct white line appears in the middle-right area, representing a scratch defect. In the difference binary image of the fifth blade, there is a horizontally placed white stripe in the upper-left edge area, and a small white area also appears in the middle-right area, both of which are not typical defects and need to be excluded. In the difference binary image of the seventh blade, there is also a small white area on the right side that needs to be excluded.

Figure 9. Differential binary images of the first, third, fourth, fifth, and seventh razor blades.

(3) Conducting morphological opening operations on the Mask was performed to reduce interference, ensuring the effectiveness of defect detection.

(4) For the convenience of visual inspection, optional binary conversion of the Mask was applied.

(5) In this study, it was assumed that the cumulative white pixel count within the ROI contour of the razor blade exceeded 50, and the area of individual white regions within the ROI was greater than 10. Thus, these conditions were considered indicative of the presence of defects. Upon analysis, the quantity of white pixels in the differential binary images of the five razor blades can be found in Table 1 (refer to Figure 10 for the detection results).

Table 1. Statistics of the number of white pixels contained in the differential binary image.

Serial number	Number of white pixels (threshold is 50)	Remark
1	84	
3	235	
4	180	
5	216	error detection
7	<50	

Figure 10. Defect detection results.

In Table 1, there are four differential binary images with more than 50 white pixels, three of which need further analysis of defect types, while the fifth one is a false detection that needs further exclusion. In the fifth differential binary image of the blade, there is a white stripe at the left upper edge on the blade. By analyzing the aspect ratio, coordinates and area of the contour, this type of false detection can be avoided. As the white area is located at the edge of the contour, it is not conducive to contour analysis, so a new mask Mask' is reconstructed based on the original mask. Mask' is wider and taller than Mask by 2 pixels in both horizontal and vertical directions (one pixel is filled on each side), and then Mask is copied to the central position of Mask' as the ROI of Mask'.

The maximum aspect ratios of the bounding rectangles of each object contour in Mask' were calculated, with a threshold of 4 assumed. Meanwhile, the y-coordinates of the upper left corners of each contour were checked. If any of them was less than 5, or if $h' - (\mathrm{y} + h) < 10$, it was excluded. In addition, contours that were located in the central region of Mask' or at the edge but not in a long strip shape were filtered based on an area threshold (assumed to be 20 in this article).

After these analyses, the statistical results of the new differential binary images Mask' of the five razor blades are presented in Table 2 (see Figure 11 for the detection results).

Table 2. Statistical results of new differential binary image Mask'.

Blade serial number	Blade internal defect serial number	Aspect ratio (threshold is 4)	Area (threshold is 20)	Number of white pixels (threshold is 50)
1	1	0.80	56.00	84
3	1	3.50	26.00	235
	2	13.00	76.00	
4	1	0.52	133.50	180
5				216
7				<50

In the new differential binary image Mask' of the third razor blade, a contour with a

width-to-height ratio of 13.00 was detected. As it was located in the central region of the image, it was identified as a scratch defect.

Figure 11. Defect detection results

3. Results and Discussion

To better test the effectiveness of the blade defect detection algorithm for razors, we deliberately selected 224 blades, including 54 blades with only scratch defects (group A), 39 blades with only damage defects (group B), 16 blades with both scratch and damage defects (group C), and 115 qualified blades (group D). Then, we conducted testing on the detection platform, and the test results are presented in Table 3.

Table 2. Razor blade defect detection experimental results.

	Scratches (Group A)	Damaged (Group B)	Scratches & damaged (Group C)	Qualified (Group D)
Total	54	39	16	115
Number of missed detections	0	0	0	
Number of false detections	0	0	1	
Complete extraction	49	38	14	
Not fully extracted	5	1	2	
Missed detection rate	0%	0%	0%	
Complete extraction rate	90.74%	97.44%	87.50%	
Total	54	39	16	115

We found through analysis that in the experimental testing process, the false negative rates for both scratch and damage defects were zero, fully meeting the requirements for defect detection. Although there was one case of misdetection in group C, through in-depth analysis, we discovered that it was due to the overlap of scratch and damage locations, resulting in only the

damage defect being detected during the testing process.

During the experiment, we observed that there were cases of incomplete extraction of defects in groups A, B, and C. The incomplete extraction rate was higher in group C. After careful observation and analysis of the incomplete defect extraction areas, we found that the main reasons for this result were as follows: some scratch defect areas were relatively small, and there were breaks in the middle of the scratches, resulting in a lower contrast compared to the qualified area. During the opening operation of morphology, these scratches may disappear, leading to incomplete extraction.

In summary, the razor blade defect detection platform can achieve detection of scratch defects and damage defects on the surface of razor blades. Although in some cases there may be incomplete extraction of defect areas, the efficiency of detection is greatly improved compared to manual detection methods. At the same time, there may be cases of misdetection during defect detection, but the detection results still identify defects, meeting the requirement of no false negatives. Therefore, it can be used in practical production.

4. Conclusions

In this paper, we propose an algorithm for surface defect detection on razor blade based on the combination of image processing and binary analysis. To achieve the detection of multiple defects simultaneously, we constructed a template model of the razor blade using frame averaging. During dynamic detection, we calculated the differences between the binary template model and each region of interest (ROI) differential binary image. By performing contour analysis on the differential binary images and eliminating edge differences, we were able to accurately identify defects such as scratches and damage.

Experimental results demonstrate that the algorithm can process the array images of razor blades obtained from cameras continuously and rapidly, and automatically detect the defect types on the razor blades. The proposed defect detection algorithm for razor blades is a potential solution for automatic visual control systems of blade quality.

However, the developed algorithm cannot recognize other defect types, such as cracks, depressions, stains, etc. Therefore, further work is needed to investigate methods for addressing the problem of defect classification and developing more advanced algorithms.

Funding: This research was funded by the Fujian Province Young and Middle-aged Teacher Education Research Project(Grant Numbers: JAS22149/JAT231113), the Major project of Fujian Provincial Social Science Research Base(Grant Number: FJ2021MJDZ029), the Sanming University Scientific Research Project(Grant Number: KD22013SP).
Institutional Review Board Statement: Not applicable.
Informed Consent Statement: Not applicable.
Data Availability Statement: Not applicable.
Conflicts of Interest: The authors declare no conflict of interest.

References

[1] Zhichao You, Hongli Gao, Liang Guo, et al. Machine vision based adaptive online condition

monitoring for milling cutter under spindle rotation [J]. Mechanical Systems and Signal Processing, 2022, 171, paper number: 108904.
[2] Guo Shuxia, Zhang Jiancheng, Jiang Xiaofeng, et al. Mini Milling Cutter Measurement Based on Machine Vision[J]. Procedia Engineering, 2011, 15:1807-1811.
[3] Ji Shanchang. Research and application of visual inspection system for large-length workpieces [D]. Wuhan: Huazhong University of Science and Technology, 2016.
[4] C. Gonzalez-Ariasa, C.C. Viafaraa, J.J. Coronadob, et al. Automatic classification of severe and mild wear in worn surface images using histograms of oriented gradients as descriptor[J]. Wear, 2019, 426-427: 1702-1711.
[5] Hou Qiulin. Research on tool detection technology based on machine vision [D]. Jinan: Shandong University, 2018.
[6] Wang Liqiang. Research on turning tool wear status detection based on machine vision [D]. Jinan: Shandong Jianzhu University, 2020.
[7] Zou Yilin. Circular blade quality inspection system based on machine vision [D]. Chengdu: University of Electronic Science and Technology of China, 2020.
[8] Cui Xudong, Cao Puxin, Wang Pingjiang. Panoramic visual inspection technology for end and side edge defects of micro drill bits [J]. Control Theory and Application, 2021, 38(01): 157-165.
[9] Jing Ruizhen. Research on tool wear classification based on workpiece surface texture[D]. Wuhan: Huazhong University of Science and Technology, 2021.
[10] Ye Zukun, Zhou Jun, Qin Chaofeng, et al. Tool wear visual detection method using cutting edge reconstruction [J]. Journal of Xi'an Jiaotong University, 2022, 56(11): 11-20.
[11] Kunpeng Zhu, Xiaolong Yu. The monitoring of micro milling tool wear conditions by wear area estimation[J]. Mechanical Systems and Signal Processing, 2017, 93:80-91.
[12] Zhichao You, Hongli Gao, Liang Guo, et al. On-line milling cutter wear monitoring in a wide field-of-view camera[J]. Wear, 2020, 460-461, paper number: 203479.
[13] P.J. Bagga, K.S. Bajaj, M.A. Makhesana, et al. An online tool life prediction system for CNC turning using computer vision techniques[J]. Materials Today:Proceedings, 2022, 62: 2689-2693.
[14] Qinghong Wan, Lai Zou, Congcong Han, et al. A U-net-based intelligent approach for belt morphology quantification and wear monitoring[J]. Journal of Materials Processing Tech, 2022, 306, paper number: 117652.
[15] Chen Chen. Tool image contour feature detection[D]. Xi'an: Xi'an University of Technology, 2013.
[16] Liang Zhibin. Research on key technologies of tool gap detection system based on machine vision [D]. Guilin: Guilin University of Electronic Science and Technology, 2021.
[17] Cheng Ying, Li Xiaofan, Zhu Ning. Research on online tool contour detection method based on machine vision [J]. Optical Technology, 2020, 46(02): 167-172.
[18] Liu Jianchun, Lin Haisen, Huang Yongjie, etc. Research on metal edge subtle defect detection methods based on machine vision [J]. Manufacturing Technology and Machine Tools, 2018, 677(11): 137-140.
[19] Zhu Qianjie. Research on surface defect detection algorithm of metal mobile phone casing based on machine vision [D]. Changsha: Hunan University, 2020.
[20] Wang Daolei, Liu Yiteng, Du Wenbin, et al. Metal surface defect detection method based on cascaded twin dense network [J]. Journal of Computer-Aided Design and Graphics, 2022, 34(06): 946-952.

[21] Xu Luyan. Tool on-machine inspection based on computer vision[D]. Tianjin: Tianjin University, 2016.
[22] Hu Junqing, Liu Ruixiang. Research on tool detection system based on image processing[J]. Internal Combustion Engine and Accessories, 2018, 16: 21-23.
[23] Yu Haichuan, Mu Pingan. Application of adaptive Canny algorithm in steel plate defect edge detection [J]. Software Guide, 2018, 17(04): 175-177.
[24] Wang Linlin. Design of micro drill bit edge quality inspection system based on machine vision [D]. Guiyang: Guizhou University, 2017.
[25] M. Sezgin and B. Sankur. Survey over image thresholding techniques and quantitative performance evaluation. Journal of Electronic Imaging. 2004, 13 (1): 146–165. doi:10.1117/1.1631315
[26] Nobuyuki Otsu. A threshold selection method from gray-level histograms. IEEE Trans. Sys., Man., Cyber. 1979, 9 (1): 62–66. doi:10.1109/TSMC.1979.4310076